Int J Biometeorol
DOI 10.1007/s00484-011-0438-1

ORIGINAL PAPER

Photographic assessment of temperate forest understory phenology in relation to springtime meteorological drivers

Liang Liang · Mark D. Schwartz · Songlin Fei

Received: 2 April 2010 / Revised: 22 February 2011 / Accepted: 22 February 2011

Abstract Phenology shows sensitive responses to seasonal changes in atmospheric conditions. Forest understory phenology, in particular, is a crucial component of the forest ecosystem that interacts with meteorological factors, and ecosystem functions such as carbon exchange and nutrient cycling. Quantifying understory phenology is challenging due to the multiplicity of species and heterogeneous spatial distribution. The use of digital photography for assessing forest understory phenology was systematically tested in this study within a temperate forest during spring 2007. Five phenology metrics (phenometrics) were extracted from digital photos using three band algebra and two greenness percentage (image binarization) methods. Phenometrics were compared with a comprehensive suite of concurrent meteorological variables. Results show that greenness percentage cover approaches were relatively robust in capturing forest understory green-up. Derived spring phenology of understory plants responded to accumulated air temperature as anticipated, and with day-to-day changes strongly affected by estimated moisture availability. This study suggests that visible-light photographic assessment is useful for efficient forest understory phenology monitoring and allows more comprehensive data collection in support of ecosystem/land surface models.

Keywords Landscape phenology · Forest understory · Temperate forest · Digital photography · EOS Land Validation Core Sites

L. Liang (✉)
Department of Forestry, University of Kentucky,
223 T.P. Cooper Bldg,
Lexington, KY 40546–0073, USA
e-mail: liang.liang@uky.edu

M. D. Schwartz
Department of Geography, University of Wisconsin-Milwaukee,
P.O. Box 413, Milwaukee, WI 53201–0413, USA
e-mail: mds@uwm.edu

S. Fei
Department of Forestry, University of Kentucky,
204 T.P. Cooper Bldg,
Lexington, KY 40546–0073, USA
e-mail: songlin.fei@uky.edu

Introduction

Phenology is the study of periodical plant and animal life cycle events as influenced by environmental factors, especially weather and climate (Schwartz 2003). Weather fluctuations and long-term climate change constantly affect the timing behaviors of biological systems. Assessments of global change impacts have identified phenology as a key indicator of ecosystem alteration (IPCC 2007; Morisette et al. 2009). Temperate forests, in particular, are important for assessing changes of ecosystem properties given the typically strong seasonality that is integral to annual temperature regimes of mid-latitude land regions. Further, understory plants form an important component influencing the general composition, nutrient cycling, and health of forests (Fei and Steiner 2008; Gilliam and Roberts 2003; Kaeser et al. 2008; Yarie 1980) and contribute to ecosystem carbon and water exchange (Drewitt et al. 2002; Pfitsch and Pearcy 1989). Phenology of understory plants is influenced by micro-environmental conditions different from that of tree canopies, and could potentially respond to climate change in unique ways within forests (Beatty 1984; Kudo et al. 2008; Rich et al. 2008). In addition, high resolution measurement of understory phenological progression allows for a more comprehensive characterization of forest vegetation dynamics, and enhances the accuracy of

Published online: 10 May 2011

validation efforts for satellite-based vegetation indices (Liang and Schwartz 2009). Given all these important aspects, more in-depth investigations are needed to further understanding of understory phenology in relation to forest ecosystem changes. Also, being able to detect detailed patterns of micrometeorological factors that influence forest understory phenology is crucial for gaining insight concerning how forest ecosystem structure might respond to global climate change.

Phenology of typical understory plants, such as grass and herb species, can be described in detail according to their respective growth stages, given sufficient observation time (Henebry 2003; Meier 1997). However, it is difficult to conduct quick repetitive observations with detailed descriptive protocols under field conditions, due to the multiplicity of species intertwined within a small area, diverse morphologies of plants, distribution heterogeneity over the forest floor, and human resource constraints. Therefore, assessment using digital cameras could provide a convenient approach to quickly capturing the green-up sequence of understory plants. In recent years, the use of networked digital cameras has been employed for regularly recording phenological changes of forest canopies (Ahrends et al. 2009; Richardson et al. 2009). Automated camera systems have also been used to record phenology of selected understory species of interest in managed environments (Crimmins and Crimmins 2008; Graham et al. 2009). To our knowledge, systematic sampling of natural forest understory phenology has only rarely been conducted, partly due to a lack of efficient approaches that would allow observers to conduct recurrent measurement and analysis for high resolution samples with desired accuracy, given the challenges mentioned above. In this study, we systematically recorded high resolution understory phenology using frequent digital photography, and tested different methods for deriving phenological metrics (phenometrics) from digital photos. Using selected phenometrics, we further examined springtime understory phenology in the context of its meteorological drivers through a focused spatiotemporal analysis.

Materials and methods

Study site description

The field work was conducted in the Chequamegon National Forest, near Park Falls, Wisconsin. The study site is located in the vicinity of a television tower (WLEF, 45.946°N, 90.272°W) which also supports AmeriFlux eddy covariance instruments, and is an Earth Observing System (EOS) Land Validation Core Site. The gentle sloping topography underlying the forest is covered with soils developed from parent materials of glacial-fluvial deposits (Martin 1965). The regional climate is humid continental with annual average temperature of 4.8°C, and annual precipitation around 810 mm (Wisconsin Online: http://www.wisconline.com/counties/price/climate.html). Forests in this limited study area are primarily composed of: (1) aspen/fir forest dominated by quaking aspen (*Populus tremuloides*) and balsam fir (*Abies balsamea*), with other species such as red maple (*Acer rubrum*) and white birch (*Betula papyrifera*); and (2) forested wetlands occupied mainly by white cedar (*Thuja occidentalis*), balsam fir, and speckled alder (*Alnus regosa*) (Ewers et al. 2002).

More than 100 understory species were identified in the forest under study (Brosofske et al. 2001). The composition of understory cover ranges from grass, sedge and herbaceous species in drier habitats, to sphagnum moss in moister habitats, often mixed with seedlings and saplings of woody species. Primary understory plants observed include species such as Canada mayflower (*Maianthemum canadense*), bunchberry dogwood (*Cornus canadensis*), dewberry (*Rubus* spp.), starflower (*Trientalis borealis*), barren strawberry (*Waldsteinia* spp.), wild strawberry (*Fragaria vesca*), groundpine (*Lycopodium dendroideum*), Virginia creeper (*Parthenocissus quinquefolia*), goldenrod (*Solidago* spp.), violet (*Viola* spp.), bedstraw (*Galium* spp.), peat moss (*Sphagnum* spp.), blueberry (*Vaccinium* spp.), woodfern (*Dryopteris* spp.), ladyfern (*Athyrium* spp.), panic grass (*Panicum* spp.), and a variety of sedges (*Carex* spp.). Seedlings and saplings found to mix with other understory plants were mainly red maple, balsam fir, and quaking aspen.

Phenology data collection

Field observation of understory vegetation phenology within the forest was conducted in spring 2007. Ground sampling was done within an approximately 625×275 m area (Fig. 1). Twenty-one 1×1 m plots were set on selected spots along existing transects outlined according to a cyclic sampling design (Burrows et al. 2002; Liang and Schwartz 2009). Sixteen of these plots followed an equally spaced systematic sampling scheme along four transects with 175-m sampling intervals. The remaining five plots were deployed randomly at additional locations empirically identified as representative ground cover types, to increase the representativeness of landscape heterogeneity. Each understory plot was laid out using a PVC pipe "square" and marked with stakes at four corners.

Digital photography was used to obtain phenological signals that represent the aggregated reflectance of multi-species green-up. Given previously mentioned challenges in regards to collecting phenological information for individual understory species, we treated the fixed-sized understory plots as basic observation units. Field work was

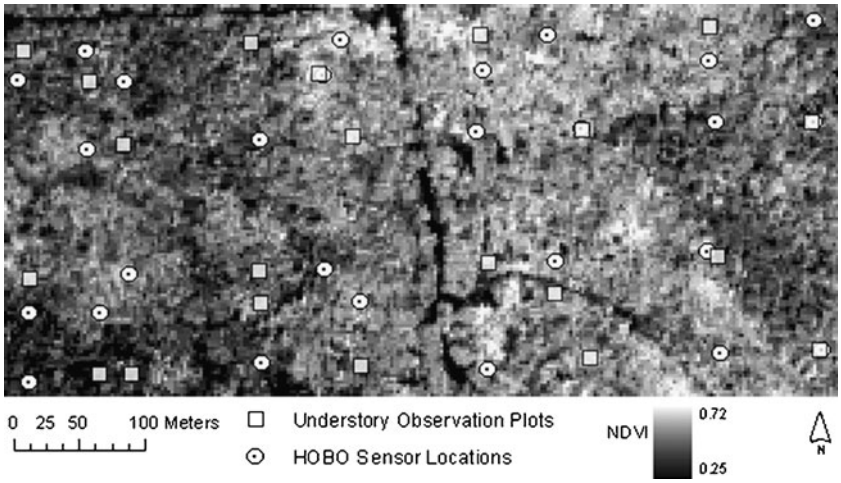

Fig. 1 Locations of understory plots and HOBO loggers overlaid on a QuickBird image-derived Normalized Difference Vegetation Index (NDVI) map showing vegetation cover conditions on May 18, 2007

conducted during the morning or before early afternoon (1300 hours) of every other day from April 29 to May 25, 2007 (14 days in total). A consumer-grade 5MP Kodak DX4530 visible-light digital camera was used. The camera had firmware version 1.0 installed and supported automatic white balance. The camera mode was set to automatic with auto-exposure enabled. Nadir-pointing images were taken over every plot at 1.5 m above the ground. The observer took care to make the images consistent position-wise under varying field conditions, and to take all images from the same height and at zenith above the ground (a sample image is shown in Fig. 2).

Meteorological measurements

Micrometeorological data were collected with HOBO data loggers (Onset Computer) deployed at 27 locations across the study area (Fig. 1). These data loggers were set to take temperature and humidity measurements of the ambient air (at standard 1.5 m shelter height) at 10-min reading intervals. Recorded data were stored in memory within each logger for later retrieval. HOBO recording was initiated on April 5, 2007 prior to the field campaign and recovered on the last day of observation (May 25, 2007). In addition to the high resolution meteorological measurements, daily precipitation data from the closest official weather station at Park Falls (approximately 8 miles, c. 13 km west of the study site) were acquired through the National Climatic Data Center (NCDC: http://www.ncdc.noaa.gov/oa/ncdc.html). The time span of these data ran from January 1 to May 31, 2007. Precipitation data were mainly used to compare with air humidity measurements which supported high resolution analysis.

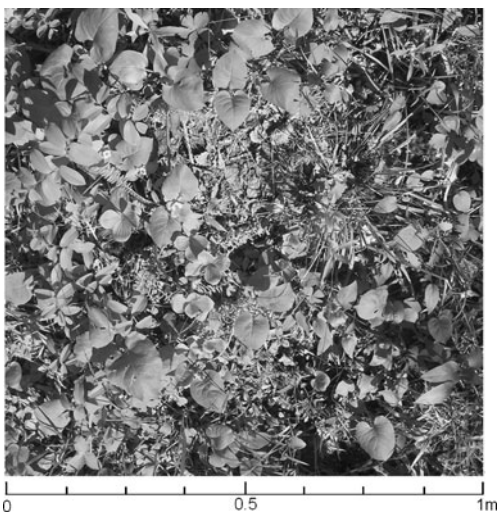

Fig. 2 A sample digital photo of an understory plot taken on May 25, 2007; cropped to contain the 1×1 m plot area (original photo is in color, presented here in gray scale)

Phenometrics derivation

A visible-light digital camera allows assessments of vegetation greening, despite the lack of a near infrared spectral band that is often indispensible for vegetation remote sensing (Jensen 2000; Lukina et al. 1999). Digital images taken with a visible-light camera natively contain separable red-green-blue (RGB) color bands. Band algebras and percentage cover estimates (image binarization) can hence be used to derive signals of plant greenness, and in turn to characterize plant phenology (Ahrends et al. 2008; Graham et al. 2006; Lukina et al. 1999; Richardson et al. 2007). Besides using native RGB bands, a recent study suggested an alternative approach based on hue-saturation-luminance (HSL) color space, which may provide more accurate estimation of plant color change by separating luminance/brightness (potentially affected by illumination conditions) from the hue (Graham et al. 2009).

The HSL color space is represented with a cylinder model. The angle around the central axis of the cylinder

corresponds to hue, which represents the color or wavelength of the pixel; the distance towards the axis corresponds to saturation which represents the purity of color, and the height of the cylinder corresponds to lightness (also referred to as intensity) which is the overall brightness of the scene as varying from black to white. The HSL color space representation can be translated from RGB color bands (Conrac Corporation 1980; ERDAS 2008; Pratt 2001) using the following equations:

$$r = \frac{M - R}{M - m}; g = \frac{M - G}{M - m}; b = \frac{M - B}{M - m} \quad (1)$$

where R, G, B are each in the range of 0–1 (converted from digital numbers); r, g, b are each in the range of 0–1 (at least one of r, g, or b values is 0, and at least one of the r, g, or b values is 1); M is the maximum value of R, G, or B, m is the minimum value of R, G, or B. Then, the lightness (L) in the range of 0–1 is computed as:

$$L = \frac{M + m}{2} \quad (2)$$

The saturation (S) in the range of 0–1 is calculated as:

$$S = 0, \text{ If} M = m \quad (3)$$

$$S = \frac{M - m}{M + m}, \text{ If } L \leq 0.5 \quad (4)$$

$$S = \frac{M - m}{2 - M - m}, \text{ If } L > 0.5 \quad (5)$$

Finally the hue (H) in the range of 0–360 is calculated as:

$$H = 0, \text{ If } M = m \quad (6)$$

$$H = 60(2 + b - g), \text{ If } R = M \quad (7)$$

$$H = 60(4 + r - b), \text{ If } G = M \quad (8)$$

$$H = 60(6 + g - r), \text{ If } B = M \quad (9)$$

Preprocessing of digital images was conducted with the Paint.NET program. ERDAS Imagine 9.2 (ERDAS 2008) was used to perform band algebra, color space transformation, and image analysis.

Each digital image was cropped to include only a 1 m^2 plot area marked out by four corner sticks. Three selected methods of combining RGB bands for phenology signal extraction were tested: (1) G/R (Graham et al. 2006); (2) 2G-R-B (Richardson et al. 2007; Woebbecke et al. 1995); and (3) (G-R) / (G+R) (Brügger et al. 2007). Mean values of the band algebra estimates were calculated for all pixels within each plot area. Percentage of green pixels was estimated according to the concept of image binarization which has wide applications in the field of pattern recognition and has been introduced into agricultural practices (Tellaeche et al. 2008; Tian and Slaughter 1998). In this study, simple threshold-based approaches were used to separate green cover from the background. For RGB bands, a criteria: G > R and G > B was applied to discriminate green pixels from the background. The HSL-based approach first converted RGB to HSL color space; then thresholds (above 192 and below 288) for green color within the hue value range (0–360) were applied. The results from both RGB- and HSL-based methods were binary images with green pixels distinguished from the background. Areal percentages of green pixels were then computed for all binary images.

Evaluating phenometrics

Inter-comparison of the resultant time series of five phenometrics was made in regards to their different temporal variability. Standardization to a 0–1 ratio was applied to averaged time series using the algorithm: (phenometric value – phenometric minimum) / (phenometric maximum – phenometric minimum). In addition to direct comparison, bi-daily increments of phenometric values were computed and compared to one another accordingly. Coefficients of variation (CV) were computed for bi-daily changes of phenometrics. We evaluated the stability which in this context indicates the performance of a phenometric in regards to capturing a realistic phenological trend. In particular, this trend refers to the green-up process which normally advances without backward development during springtime, unless affected by disturbances such as insect outbursts or grazing, or by excessive deprivation of required resources. Our basic assumption suggests that a stable phenometric representation should reflect a steady increase in greenness during the early spring under disturbance-free conditions. Throughout the observation time period, no disturbances from wildlife were noticed and all plots remained intact. Given these considerations, we expected the phenometrics derived to match the consistently upturning spring green-up process. Consequently, downward departures from a previous greenness level as indicated by negative bi-daily changes would suggest measurement instability. We therefore used this criterion to infer the relative robustness of the five phenometrics derived against potential errors and measurement uncertainties. More stable phenometrics were selected in support of subsequent analysis regarding meteorological drivers.

Processing meteorological variables

High frequency/intensity temperature and humidity measurements allowed detailed characterization of micrometeorological conditions. We first computed temperature and humidity indices (daily maximum, mean, and minimum) averaged over the entire study area. These indices were compared with precipitation data recorded at the nearby official weather station. Pearson correlation coefficients were calculated for precipitation and air humidity indices, including both absolute humidity and relative humidity. For high resolution analysis, field-measured temperature, absolute humidity, and relative humidity data were interpolated to understory plot locations using ordinary Kriging. Daily temperature and humidity indices (maximum, mean, and minimum) for each plot were then computed. Accumulated growing degree hours (AGDH) were calculated from hourly mean temperature based on a −0.6°C threshold (Schwartz 1997) starting from April 5, 2007. It was assumed that chilling requirement necessary for dormancy release (Schwartz 1997; Simpson 1990) was fulfilled prior to this date. In order to perform a more comprehensive examination of potential meteorological drivers, air water potential and vapor pressure deficit were calculated from temperature and relative humidity (Buck 1981; Kirkham 2004; Lambers et al. 1998), and included in the analysis. Accumulated humidity indices were derived from hourly means of measurements in like manner as AGDH. Given that understory observations were taken bi-daily, "cross-day change" (a prior day measure subtracts the value from the day before) of all meteorological variables was calculated. Lastly, antecedent 2-day accumulations of temperature and humidity were computed in order to provide a short-term analysis of accumulated meteorological conditions. A list of the meteorological variables used in the study is provided in Table 1. Climate data interpolation, processing and analysis were performed using R (R Development Core Team 2009).

Examining meteorological drivers

Understory phenology was compared with both long-term and short-term meteorological conditions as described by a comprehensive suite of variables (see Table 1 for details). In addition to cumulative phenology, changes of phenometric values between two consecutive bi-daily observations were calculated for each plot to correspond with day-to-day weather fluctuations. Meteorological drivers of understory phenology were examined using linear multiple regression analysis. At the plot level, our field data represented a panel data structure with multi-date observations from a group of fixed targets, with both temporal and spatial dimensions. In order to accommodate such a data structure, linear multiple regression models were fitted to data using a panel linear model (*plm*) package in R (Croissant and Millo 2008). Phenometrics at each plot were self-standardized by dividing an original value by the site-specific range (i.e., site maximum minus site minimum) to reduce site variability related to species composition diversity. Both standardized and raw datasets were regressed against meteorological variables. For cumulative phenological time series, accumulated hourly means of temperature, absolute humidity, relative humidity, water potential, and vapor pressure deficit were used as candidate explanatory variables. Phenological changes between two consecutive observations were modeled with additional variables representing daily weather conditions, antecedent weather conditions, and cross-day weather changes.

Variable subset selection was first conducted for each variable group (such as temperature-based variables or absolute humidity-based variables) using an exhaustive search approach supported by an R package: *leaps* (Miller 2002). The *leaps* package returns variable subsets with data multicollinearity minimized. Bayesian information criterion (BIC, provided in the *leaps* package in R) was used to determine the best variable subsets with overfitting avoided. Variables chosen from different groups were combined for a further-step selection via the same approach as described above. Final subsets of variables were then used to fit linear panel data regression models. A logarithmic transformation was applied to selected variables before model building to correct heteroscedasticity in the data. Hausman test (provided with the *plm* package in R) was performed to decide whether a fixed or random effect sub-model was appropriate. Finally, models with all coefficients significant at the 99% confidence level were retained. In addition to plot level analysis, phenometrics averaged across plots over the entire study area were compared with averaged meteorological variables using ordinary least squares linear models. Averaged variables represented overall conditions of the entire landscape; therefore, they are also referred to as landscape-level measures.

Results

Comparison of phenometrics

The five derived phenometrics demonstrated differing degrees of variability over time (Fig. 3; Table 2). Standardization of phenometric time series to a range between 0 and 1 allowed effective visual contrast in a unified scale frame, emphasizing their respective temporal response patterns. The among-metric differences were clearly seen in the variability of their bi-daily changes (Fig. 4). Among the

Table 1 Summary of meteorological variables used in the analysis

	Temperature (°C)	Absolute humidity (g/m3)	Relative humidity (%)	Air water potential (MPa)	Vapor pressure deficit (kPa)
Daily mean	Tmean	AHmean	RHmean	WPmean	VPDmean
Daily minimum	Tmin	AHmin	RHmin	WPmin	VPDmin
Daily maximum	Tmax	AHmax	RHmax	WPmax	VPDmax
Daily sum of hourly means	GDH	AHsum	RHsum	WPsum	VPDsum
Accumulated hourly means	AGDH	AHcum	RHcum	WPcum	VPDcum
"Cross-day change"(a prior day measure subtracts the measure of the day before)	TmeanCg	AHmeanCg	RHmeanCg	WPmeanCg	VPDmeanCg
	TminCg	AHminCg	RHminCg	WPminCg	VPDminCg
	TmaxCg	AHmaxCg	RHmaxCg	WPmaxCg	VPDmaxCg
	GDHCg	AHsumCg	RHsumCg	WPsumCg	VPDsumCg
Antecedent 2-day accumulation	GDHPre2	AHsumPre2	RHsumPre2	WPsumPre2	VPDsumPre2

T Temperature, *AH* absolute humidity, *RH* relative humidity, *WP* water potential, *VPD* vapor pressure deficit, *Cg* "Cross-day Change" indicates the meteorological change occurred from the day before yesterday to yesterday in regards to an observation day

band algebra-based phenometrics, bi-daily advance of band differencing (2G-R-B, excess green) and normalized difference ratio ([G−R]/[G+R]) showed frequent negative change values over time. Coefficients of variation (CV) of these two phenometrics were 268.03 and 178.85% respectively, greater than that of the other three phenometrics. The simple band ratio (G/R) time series demonstrated negative departures as well, yet at a smaller degree compared with the last two metrics, with a CV value of 128.42%. As detailed previously, such phenomenon likely indicate instability of these band algebra-based metrics against potential noise and measurement uncertainty, given that observed plant phenology consistently advanced during the study time period. Two greenness percentage measures demonstrated mostly positive increments over time with smaller CV values (103.30 and 102.58%, respectively) compared to band algebra-based phenometrics. And, noticeably, RGB-based and HSL-based greenness percentage metrics resemble each other in regards to the phenological progression and patterns of bi-daily change. Hence, the two greenness percentage based phenometrics appeared to be more robust against potential errors in capturing a realistic green-up process, and were adopted for subsequent evaluation of meteorological drivers.

Meteorological drivers of understory phenology

Humidity variables correlated with weather station precipitation records significantly (Table 3). Correlation coefficients with precipitation for both mean absolute humidity and relative humidity (r=0.44, and 0.61 ,respectively) were significant at the 95% confidence level. In particular, maximum absolute humidity (AHmax), and minimum relative humidity (RHmin) showed highest correlations (r=0.68, and 0.68 ,respectively) with precipitation (significant at 99% confidence level). Further, humidity fluctuations appeared to correspond with the timing and magnitude of precipitation occurrences on day-of-year (DOY) 128, 134–137, 139, 141, and 143–145 (Fig. 5). Given the significant correlations and temporal correspondence between precipitation and air humidity, field-measured humidity data were used in characterizing the general moisture availability in relation to understory growth in the below canopy environment for high resolution analysis. Besides, peak temperatures were found to occur often on the first days of rainy periods

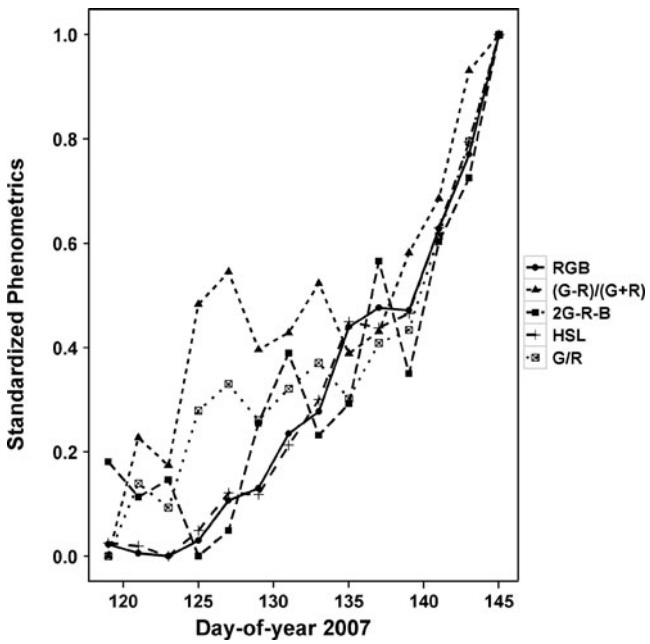

Fig. 3 Spring time series of understory phenometrics averaged across plots; derived from five different photographic methods: 1) RGB-based greenness percentage; 2) (G-R)/(G+R); 3) 2G-R-B; 4) HSL-based greenness percentage; and 5) G/R ratio (all phenometric values were standardized)

Table 2 Averaged values of phenometrics across plots with standard deviation (σ)

DOY	RGB (%)		(G−R)/(G+R)		2G-R-B (DN)		HSL(%)		G/R	
	Mean	σ	Mean	σ	Mean	σ	Mean	σ	Mean	σ
119	9.98	5.72	−0.09	0.04	−5.31	7.62	6.91	4.17	0.87	0.05
121	9.44	3.73	−0.07	0.03	−8.42	8.50	6.75	2.83	0.89	0.04
123	9.26	4.90	−0.08	0.03	−6.90	9.14	6.22	3.44	0.88	0.05
125	10.20	6.84	−0.06	0.01	−13.62	11.67	7.58	4.15	0.90	0.02
127	12.60	7.53	−0.05	0.01	−11.35	12.36	9.58	4.57	0.91	0.02
129	13.32	6.71	−0.06	0.03	−1.92	13.99	9.50	5.01	0.90	0.04
131	16.61	7.87	−0.06	0.03	4.26	11.63	12.12	6.11	0.91	0.06
133	17.94	9.64	−0.05	0.02	−2.97	12.67	14.55	7.32	0.92	0.04
135	23.02	9.26	−0.06	0.02	−0.19	17.11	18.70	7.20	0.91	0.03
137	24.18	11.51	−0.06	0.04	12.35	15.88	18.38	9.13	0.92	0.07
139	24.02	9.67	−0.05	0.01	2.46	17.01	19.14	8.18	0.93	0.02
141	28.91	13.82	−0.04	0.03	14.10	22.90	23.70	11.88	0.95	0.06
143	33.39	15.48	−0.03	0.03	19.70	28.76	28.28	12.67	0.97	0.06
145	40.57	15.25	−0.02	0.03	32.32	26.39	33.98	12.53	1.00	0.07

DOY Day of year, *DN* digital number

(such as DOY 134 and 143), followed by immediate temperature declines. In addition, bi-daily increments of phenometric values demonstrated temporal correspondences with increases of precipitation and humidity (Figs. 4 and 5). Especially for greenness percentage based phenometrics, accelerated increments were found on DOY 135 and 145 which were preceded by DOY134 and 144 when considerable amounts of precipitation occurred. An exception was that during the early part of spring season, a single precipitation event on DOY 128 did not seem to match up with any observed phenological advance.

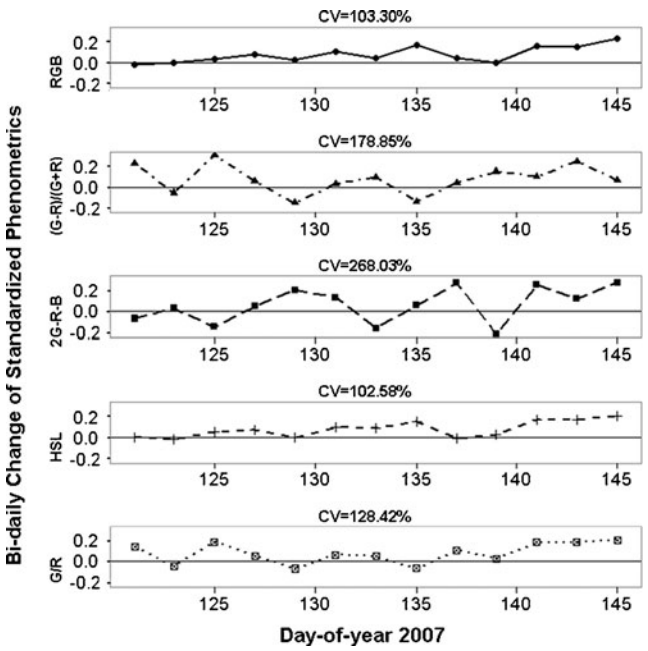

Fig. 4 Bi-daily changes of spring time series of understory phenometrics averaged across plots as derived from the five different photographic methods; *CV* coefficient of variation

For cumulative phenology, fitted panel linear models implied that understory green-up responded to both temperature and humidity strongly. All models were significant at the 99% confidence level (Table 4). Results revealed that accumulated growing degree hours (AGDH) alone could drive a model with a coefficient of determination greater than 0.60. Yet humidity-based variables, accumulated vapor pressure deficit (VPDcum), or the accumulated absolute humidity (AHcum), were also significant explanatory variables. Models with humidity-based variables added significantly raised their explanatory powers. RGB-based phenometrics were consistently better predicted with meteorological variables than HSL-based phenometrics. Further, standardization appeared to raise the explanatory power of models for RGB-based phenometrics in most cases, but only improved one case among models using HSL-based phenometrics. Plotting the identified meteorological drivers respectively against phenometrics, a linear dependency can be clearly seen in all cases (Fig. 6).

Panel linear models fitted for incremental phenological change underperformed that of cumulative phenometrics at the plot level. A few plot-level incremental phenology models were significant at confidence levels up to 99%. However, all model coefficients of determination were below 0.20. Therefore, analyzing meteorological drivers of phenological change relied on landscape-level models, fitted with phenometrics and meteorological variables averaged across the entire study area. The landscape-level values here simply indicate the averaged understory phenometrics and meteorological conditions, with inter-plot variations smoothed. According to landscape-level

Table 3 Correlations between precipitation and air humidity variables

		AHmax	AHmin	AHmean	RHmax	RHmin	RHmean
PREC	Pearson's *r*	0.68	0.35	0.44	0.31	0.68	0.61
	p value	<0.001	0.066	0.016	0.103	<0.001	<0.001

PREC Precipitation, *AH* absolute humidity, *RH* relative humidity

linear regression models, incremental phenology could be explained by AGDH, AHcum, or a combination of daily maximum vapor pressure deficit (VPDmax) and antecedent 2-day absolute humidity accumulation (AHsumPre2), respectively (Table 5). All the models were significant at the 99% confidence level. The first two models with either AGDH or AHcum as the predictor variable were similar in their explanatory powers (R^2=0.512-0.518). Models driven by VPDmax and AHsumPre2 were considerably stronger with coefficients of determination improvement ranging from 0.17 to 0.30 in comparison with models with long-term accumulated measures (AGDH, or AHcum) as predictors. Investigated separately in scatter plots with linear fit lines, phenological change was positively dependent on AGDH, AHcum, or AHsumPre2, and negatively dependent on VPDmax (Fig. 7). Humidity-based variables could explain phenological change independently of AGDH. This was unlike the relationship with cumulative phenometrics, which required AGDH in all models. To summarize, cumulative phenology was reasonably well predicted by thermal time (AGDH), but as far as the increment of phenological progression is concerned, humidity-based indices manifested themselves as independent explanatory factors. In addition, we found that standardized phenometrics only out-performed non-standardized metrics for models driven by VPDmax and AHsumPre2, but with reduced effects on the models driven by AGDH or AHcum. In the case of landscape-level analysis, RGB- and HSL-based phenometrics did not show marked differences overall as far as the explanatory power of models is concerned, except that HSL-based models performed better than the RGB-based for the standardized phenometrics.

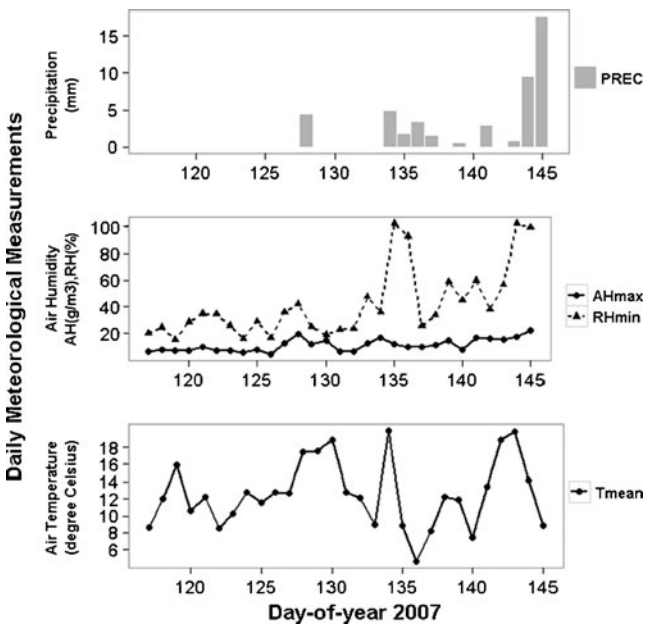

Fig. 5 Spring time series of daily meteorological measurements (*PREC* precipitation in mm, *AHmax* maximum absolute humidity in g/m^3, *RHmin* minimum relative humidity in %, *Tmean* mean temperature in °C)

Discussion

The greening of understory plants forms an important aspect of temperate forest seasonal dynamics. As shown in this study, digital photography is useful for more accurate repeated measurement of understory phenology. Among the five phenometrics derived from digital photos, greenness percentage estimates were more robust against potential errors than band algebra-based metrics, although band algebra-based methods may be indispensible for characterizing vegetation change over fully covered plots. The potential errors that caused the instability of phenometrics may stem mainly from illumination variability across plots and uncertainties of the camera system. Different site canopy characteristics, sun angle/position, and cloud condition at the time of observation unavoidably affected the reflectance from understory. The digital camera with auto-exposure enabled also increased the inconsistency of photos taken for different plots at different times, yet it may have balanced off the variability of light conditions to a certain degree. Nevertheless, the greenness percentage approach appeared to be less sensitive to such uncertainties, and provided more realistic phenological progression signals.

Greenness percentage estimates from RGB and HSL color spaces responded to meteorological variables sensitively. The HSL-based phenometric was considered more accurate given its ability to reduce errors caused by illumination variability (Graham et al. 2009). In this study, according to regression model performance, RGB-based phenometric appeared to be more responsive to micrometeorological variations across plots than the HSL-based.

Table 4 Panel linear models of plot-level phenometrics

Phenometrics	Explanatory variables and coefficients	R^2	p value
HSL	AGDH (1.540)	0.650	<0.001
HSL	AGDH (4.890), VPDcum (−4.444)	0.694	<0.001
HSL	AGDH (−1.276), AHcum (3.018)	0.676	<0.001
HSL_S	AGDH (1.539)	0.650	<0.001
HSL_S	AGDH (4.890), VPDcum (−4.444)	0.694	<0.001
HSL_S	AGDH (−1.616), AHcum (3.381)	0.695	<0.001
RGB	AGDH (1.345)	0.715	<0.001
RGB	AGDH (4.417), VPDcum (−4.073)	0.755	<0.001
RGB	AGDH (−1.769), AHcum (3.337)	0.760	<0.001
RGB_S	AGDH (1.344)	0.714	<0.001
RGB_S	AGDH (4.654), VPDcum (−4.388)	0.770	<0.001
RGB_S	AGDH (−1.887), AHcum (3.463)	0.774	<0.001

HSL-based phenometric (*HSL*) and RGB-based phenometric (*RGB*), both represented with greenness percentage cover. The postfix *S* indicates that the variable was standardized. The explanatory meteorological variables are: accumulated growing degree hours (*AGDH*), accumulated vapor pressure deficit (*VPDcum*), and accumulated absolute humidity (*AHcum*). All coefficients of explanatory variables were significant at the 99% confidence level (p values of respective coefficients are not presented here). A log transformation was applied to all variables to correct heteroscedasticity

But among the landscape-level models created for averaged variables, standardized HSL-based phenometric supported better predictions. Given error sources discussed previously, as well as additional uncertainties from interpolation of climate data, further assessment is still needed to better compare phenometrics estimated using the two-color models.

The assessment of meteorological variables revealed detailed patterns of temperature and humidity in influencing

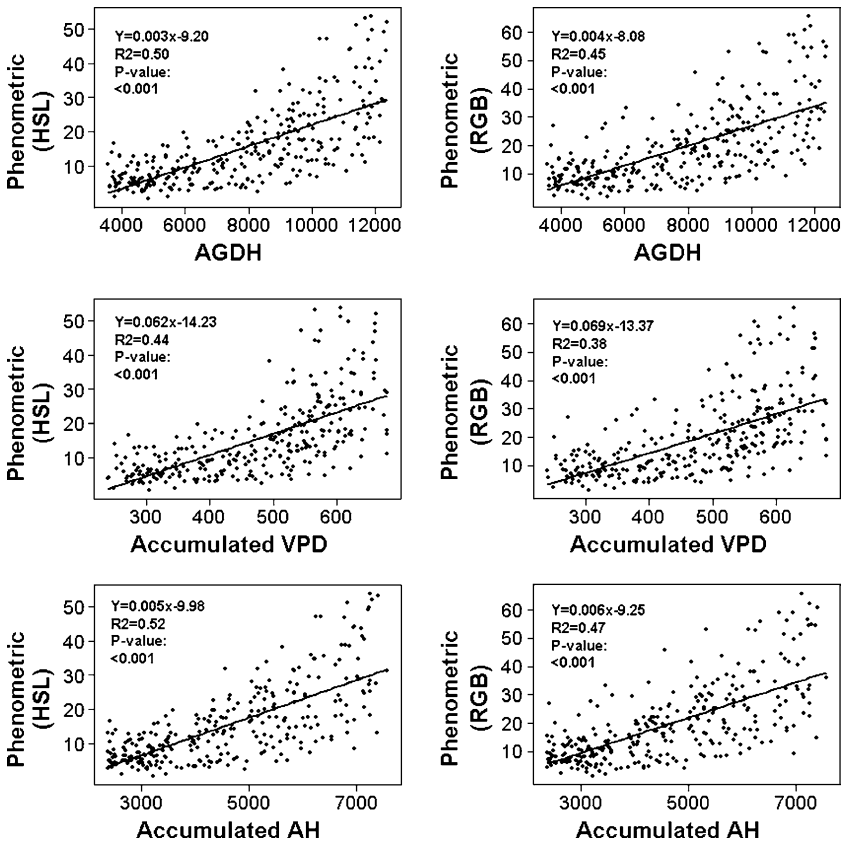

Fig. 6 Meteorological drivers of plot-level understory phenology: HSL- and RGB-based phenometrics in percentage against identified meteorological drivers: accumulated growing degree hours (*AGDH*), accumulated vapor pressure deficit (*VPD*, in kPa), and accumulated absolute humidity (*AH*, in g/m^3); regression model functions, coefficients of determination and p values are provided. Heteroscedasticity shown in the data was corrected in models using a log transformation

Table 5 Linear models of landscape-level phenometrics averaged over the study area

Models	R^2	p value
HSL.inc=0.0006 × AGDH − 2.963	0.516	0.006
HSL.inc=0.001 × AHcum − 2.947	0.516	0.006
HSL.inc=−1.802 × VPDmax + 0.008 × AHsumPre2 + 1.448	0.690	0.003
HSL_S.inc=0.00002 × AGDH − 0.107	0.508	0.006
HSL_S.inc=0.00004 × AHcum − 0.107	0.514	0.006
HSL_S.inc=−0.065 × VPDmax + 0.0003 × AHsumPre2 + 0.035	0.794	<0.001
RGB.inc=0.007 × AGDH − 3.370	0.512	0.006
RGB.inc=0.001 × AHcum − 3.382	0.518	0.006
RGB.inc=−1.699 × VPDmax + 0.012 × AHsumPre2 + 0.110	0.750	<0.001
RGB_S.inc=0.00002 × AGDH − 0.112	0.479	0.009
RGB_S.inc=0.00004 × AHcum − 0.113	0.486	0.008
RGB_S.inc=0.057 × VPDmax + 0.0004 × AHsumPre2 − 0.004	0.780	<0.001

HSL.inc The increment of HSL-based phenometric, *RGB.inc* the increment of RGB-based phenometric. The postfix *S* indicates that the variable was standardized. The explanatory meteorological variables are: accumulated growing degree hours (*AGDH*), accumulated absolute humidity (*AHcum*), maximum vapor pressure deficit (*VPDmax*), and antecedent 2-day absolute humidity accumulation (*AHsumPre2*)

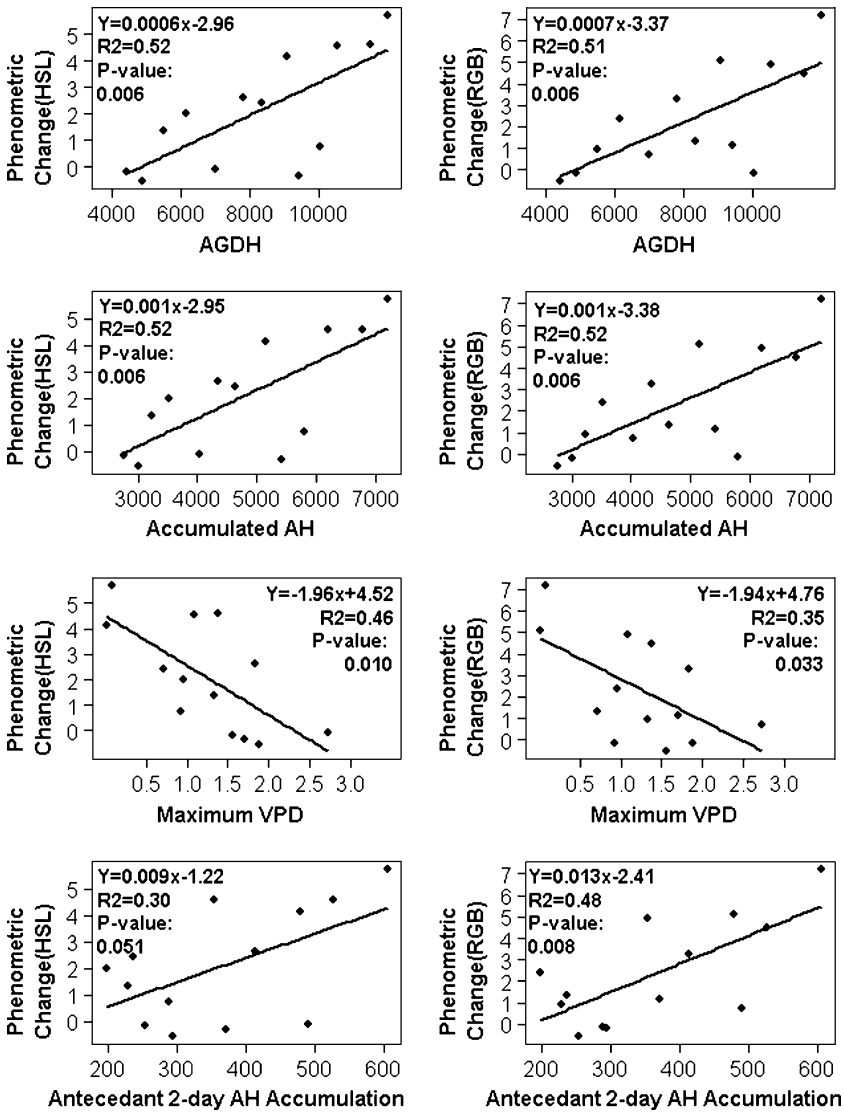

Fig. 7 Meteorological drivers of landscape-level (averaged across plots) understory phenological change; HSL- and RGB-based phenometric change (between two consecutive bi-daily observations) in percentage plotted against meteorological drivers: accumulated growing degree hours (*AGDH*), accumulated absolute humidity (*AH*, in g/m^3), daily maximum vapor pressure deficit (*VPD*, in kPa), and antecedent 2-day absolute humidity (*AH*, in g/m^3) accumulation; regression functions, coefficients of determination and p values are provided

understory plant phenology. Given the close relationship found between precipitation and air humidity, variables derived from the latter were used to indirectly indicate moisture availability. Variations of cumulative understory phenology at plot level were affected by accumulated moisture in addition to accumulated heat. Incremental phenology responded to heat and moisture accumulation, yet had stronger dependency on daily short-term change of moisture conditions. Such relationships first indicate a generally accelerated rate of understory flushing with increased spring warmth and water availability. Furthermore, they suggest that the occurrence of understory phenological change was more directly triggered by precipitation events (as reflected by humidity increase at plot level) than rising temperatures. Therefore, while accumulated heat and moisture provided a baseline for predicting spring growth of understory plants, day-to-day moisture conditions determined the actual occurrence of phenological advance.

This detected phenomenon may be related to a relatively dry spring in the study area during the year of observation. From January to May 2007, total precipitation in the area was 198 mm, which was 38 mm below the historical average (1971–2000) of 236 mm during that 5-month period of the year. The relatively dry weather mainly occurred in May (total 50 mm of precipitation) which fell far short of the historical average of 80 mm. Hence, water was a limiting resource that hindered spring green-up of understory plants during the time of observation. In a mesic forest such as that investigated in this project, shallower root systems of understory species could be a direct cause of a stronger reliance on precipitation, especially during drought spells, in line with the typical cases in semi-arid ecosystems (Brown and de Beurs 2008; Henebry 2003) and even tropical moist forests (Wright 1991). This finding further demonstrates the usefulness of photographic assessment for capturing detailed understory phenology information.

We identified the following limitations and drawbacks in relation to meteorological driver assessment. First, due to a lack of soil moisture data, air humidity was employed as a proxy for moisture availability. Although both absolute humidity and relative humidity were found to be significantly correlated with precipitation, this measurement was indirect and a large uncertainty may exist. This may be provisionally workable under conditions where air humidity change is closely connected to soil moisture variation due to precipitation and evapotranspiration within the near-ground environment (Rosenberg 1983). But in different environments where soil moisture and air humidity depart from each other significantly, such as in extreme cases of irrigated land in semiarid regions/dry seasons, using air humidity in place of direct measurement of soil water content would be inadequate. The relationship between understory phenology and meteorology could have been more precisely predicted if soil moisture and/or site specific precipitation data were available. Besides, light condition changes in the below canopy environment not only impose challenges on field observations but may also influence understory phenology directly (Kato and Komiyama 2002; Koizumi and Oshima 1985). Thus, monitoring additional environmental factors such as soil moisture and canopy shading effects is needed for a better understanding of micrometeorological factors influencing understory phenology.

Changes in understory phenology constantly affect forest ecosystems in terms of nutrient/energy cycling, species interactions, and community structures (Gilliam and Roberts 2003; Kudo et al. 2008). Accurate quantification of understory phenology can facilitate investigations into issues such like response of woody–herbaceous ecosystems to climate change and disturbances (Rich et al. 2008), forest management associated with tree regeneration and forest structure dynamics (Augspurger and Bartlett 2003; Kaeser et al. 2008), and invasive species detection (Wilfong et al. 2009). In addition, incorporating high resolution understory phenology measurements helps improve the accuracy of forest landscape phenology models for validating satellite phenology signals (Liang et al. 2011), and in turn it may improve land surface parameterizations for climate models (Bonan 2008).

Conclusions

Visible-light digital photography accompanied with greenness extraction methods provides a way to effectively collect phenological information from the forest understory, as well as similar vegetation types. Given the drawbacks related to labor intensity and systematic inconsistency, observer-based digital photography measurement could be employed as a supplementary tool to existing canopy-observing systems using fixed automatic cameras (Ahrends et al. 2009; Richardson et al. 2009). We identified percentage cover-based phenometrics as being better for capturing phenological progression against measurement uncertainties. The sensitivity of these phenometrics to subtle changes of meteorological variables supports applying this technique to monitoring understory phenology shift caused by climate change. In the context of landscape phenology, high resolution data with spatio-temporal analysis (as demonstrated in this study) are needed for detailed investigation of vegetation–climate interactions. Lastly, this easily-implemented photographic approach could potentially encourage researchers, foresters, park rangers, and citizen scientists to readily collect phenology data digitally in support of vegetation change studies and modeling.

Acknowledgements Eric Graham provided insight regarding digital photo processing. Danlin Yu provided important advice on data analysis. Geoffrey M. Henebry reviewed the manuscript and offered valuable comments. Yanbing Zheng provided valuable support in statistical analysis. Thomas Barnes helped identifying understory plant species. We also thank the five anonymous reviewers who provided constructive comments. The research was partly supported by a National Science Foundation Doctoral Dissertation Research Improvement Grant, BCS-0703360.

References

Ahrends H, Brügger R, Stöckli R, Schenk J, Michna P, Jeanneret F, Wanner H, Eugster W (2008) Quantitative phenological observations of a mixed beech forest in northern Switzerland with digital photography. J Geophys Res 113:G04004. doi:10.1029/2007JG000650

Ahrends H, Etzold S, Kutsch W, Stoeckli R, Bruegger R, Jeanneret F, Wanner H, Buchmann N, Eugster W (2009) Tree phenology and carbon dioxide fluxes: use of digital photography for process-based interpretation at the ecosystem scale. Clim Res 39:261–274

Augspurger C, Bartlett E (2003) Differences in leaf phenology between juvenile and adult trees in a temperate deciduous forest. Tree Physiol 23:517–525

Beatty S (1984) Influence of microtopography and canopy species on spatial patterns of forest understory plants. Ecology 65:1406–1419

Bonan G (2008) Forests and climate change: forcings, feedbacks, and the climate benefits of forests. Science 320:1444–1449

Brosofske K, Chen J, Crow T (2001) Understory vegetation and site factors: implications for a managed Wisconsin landscape. For Ecol Manag 146:75–87

Brown M, de Beurs K (2008) Evaluation of multi-sensor semi-arid crop season parameters based on NDVI and rainfall. Remote Sens Environ 112:2261–2271

Brügger R, Studer S, Stöckli R (2007) Die Vegetationsentwicklung-erfasst am Individuum und über den Raum (Changes in plant development-monitored on the individual plant and over geographical area). Schweiz Z Forstwes 158:221–228

Buck A (1981) New equations for computing vapor pressure and enhancement factor. J Appl Meteorol 20:1527–1532

Burrows S, Gower S, Clayton M, Mackay D, Ahl D, Norman J, Diak G (2002) Application of geostatistics to characterize Leaf Area Index (LAI) from flux tower to landscape scales using a cyclic sampling design. Ecosystems 5:667–679

Conrac Corporation (1980) Raster graphics handbook. Van Nostrand Reinhold, New York

Crimmins M, Crimmins T (2008) Monitoring plant phenology using digital repeat photography. Environ Manag 41:949–958

Croissant Y, Millo G (2008) Panel data econometrics in R: the plm package. J Stat Softw 27:1–43

Drewitt G, Black T, Nesic Z, Humphreys E, Jork E, Swanson R, Ethier G, Griffis T, Morgenstern K (2002) Measuring forest floor CO2 fluxes in a Douglas-fir forest. Agric For Meteorol 110:299–317

ERDAS (2008) ERDAS imagine field guide. ERDAS, Atlanta

Ewers B, Mackay D, Gower S, Ahl D, Burrows S, Samanta S (2002) Tree species effects on stand transpiration in northern Wisconsin. Water Resour Res 38(7):1–11

Fei S, Steiner K (2008) Relationships between advance oak regeneration and biotic and abiotic factors. Tree Physiol 28:1111–1119

Gilliam F, Roberts M (2003) The herbaceous layer in forests of eastern North America. Oxford University Press, New York

Graham EA, Hamilton MP, Mishler BD, Rundel PW, Hansen MH (2006) Use of a networked digital camera to estimate net CO2 uptake of a dessication-tolerant moss. Int J Plant Sci 167:751–758

Graham EA, Yuen EM, Robertson GF, Kaiser WJ, Hamilton MP, Rundel PW (2009) Budburst and leaf area expansion measured with a novel mobile camera system and simple color thresholding. Environ Exp Bot 65:238–244

Henebry GM (2003) Grasslands of the North American great plains. In: Schwartz MD (ed) Phenology: an integrative environmental science. Kluwer, Dordrecht, pp 157–174

IPCC (2007) Climate change 2007: the physical science basis. Contribution of working group I to the fourth assessment report of the Intergovernmental Panel on Climate Change. Solomon S, Qin D, Manning M, Chen Z, Marquis M, Averyt KB, Tignor M, Miller HL (eds). Cambridge University Press, Cambridge

Jensen JR (2000) Remote sensing of the environment: an earth resource perspective. Prentice Hall, Upper Saddle River

Kaeser M, Gould P, McDill M, Steiner K, Finley J (2008) Classifying patterns of understory vegetation in mixed-oak forests in two ecoregions of pennsylvania. Northern J Appl For 25:38–44

Kato S, Komiyama A (2002) Spatial and seasonal heterogeneity in understory light conditions caused by differential leaf flushing of deciduous overstory trees. Ecol Res 17:687–693

Kirkham M (2004) Principles of soil and plant water relations. Elsevier, Amsterdam

Koizumi H, Oshima Y (1985) Seasonal changes in photosynthesis of four understory herbs in deciduous forests. J Plant Res 98:1–13

Kudo G, Ida T, Tani T (2008) Linkages between phenology, pollination, photosynthesis, and reproduction in deciduous forest understory plants. Ecology 89:321–331

Lambers H, Chapin F, Pons T (1998) Plant physiological ecology. Springer, New York

Liang L, Schwartz MD (2009) Landscape phenology: an integrative approach to seasonal vegetation dynamics. Landsc Ecol 24:465–472

Liang L, Schwartz M, Fei S (2011) Validating satellite phenology through intensive ground observation and landscape scaling in a mixed seasonal forest. Remote Sens Environ 115:143–157

Lukina EV, Stone ML, Raun WR (1999) Estimating vegetation coverage in wheat using digital images. J Plant Nutr 22:341–350

Martin L (1965) Physical geography of Wisconsin. University of Wisconsin Press, Madison

Meier U (1997) Growth stages of mono-and dicotyledonous plants: BBCH-monograph. Federal Biological Research Centre for Agriculture and Forestry, Braunschweig

Miller A (2002) Subset selection in regression. Chapman & Hall, New York

Morisette JT, Richardson AD, Knapp AK, Fisher JI, Graham EA, Abatzoglou J, Wilson BE, Breshears DD, Henebry GM, Hanes JM, Liang L (2009) Tracking the rhythm of the seasons in the face of global change: phenological research in the 21st century. Front Ecol Environ 7:253–260

Pfitsch W, Pearcy R (1989) Daily carbon gain by Adenocaulon bicolor (Asteraceae), a redwood forest understory herb, in relation to its light environment. Oecologia 80:465–470

Pratt W (2001) Digital image processing. Wiley, New York

R Development Core Team (2009) R: a language and environment for statistical computing. R Foundation for Statistical Computing, Vienna, Austria. http://www.R-project.org

Rich P, Breshears D, White A (2008) Phenology of mixed woody-herbaceous ecosystems following extreme events: net and differential responses. Ecology 89:342–352

Richardson AD, Jenkins JP, Braswell BH, Hollinger DY, Ollinger SV, Smith ML (2007) Use of digital webcam images to track spring green-up in a deciduous broadleaf forest. Oecologia 152:323–334

Richardson AD, Braswell BH, Hollinger DY, Jenkins JP, Ollinger SV (2009) Near-surface remote sensing of spatial and temporal variation in canopy phenology. Ecol Appl 19:1417–1428

Rosenberg NJ (1983) Microclimate: the biological environment, 2nd edn. Wiley, New York

Schwartz MD (1997) Spring index models: an approach to connecting satellite and surface phenology. In: Lieth H, Schwartz MD (eds) Phenology of seasonal climates I. Backhuys, Netherlands, pp 23–38

Schwartz MD (2003) Phenology: an integrative environmental science. Kluwer, Dordrecht

Simpson G (1990) Seed dormancy in grasses. Cambridge University Press, Cambridge

Tellaeche A, BurgosArtizzu X, Pajares G, Ribeiro A, Fernández-Quintanilla C (2008) A new vision-based approach to differential spraying in precision agriculture. Comput Electron Agric 60:144–155

Tian L, Slaughter D (1998) Environmentally adaptive segmentation algorithm for outdoor image segmentation. Comput Electron Agric 21:153–168

Wilfong B, Gorchov D, Henry M (2009) Detecting an invasive shrub in deciduous forest understories using remote sensing. Weed Sci 57:512–520

Woebbecke D, Meyer G, Von Bargen K, Mortensen D (1995) Color indices for weed identification under various soil, residue, and lighting conditions. Trans ASAE 38:259–269

Wright S (1991) Seasonal drought and the phenology of understory shrubs in a tropical moist forest. Ecology 72:1643–1657

Yarie J (1980) The role of understory vegetation in the nutrient cycle of forested ecosystems in the mountain hemlock biogeoclimatic zone. Ecology 61:1498–1514